ELSEVIER

Biochimica et Biophysica Acta 1229 (1995) 39–48

BBA Biochimica et Biophysica Acta

Study on the energy transfer processes in phycobilisomes from blue-green algae by the use of stochastic simulation approach

Jingquan Zhao *, Jinchang Zhu, Lijin Jiang

Institute of Photographic Chemistry, Academia Sinica, Beijing, 100101, China

Received 19 April 1994; revised 2 November 1994; accepted 15 November 1994

Abstract

A more natural model is used for simulating the energy transfer processes in phycobilisomes from cyanobacteria. In the model, the crystal structure data of C-phycocyanins are applied and the linker polypeptides are taken into account to calculate Förster transfer rates between neighboring disks. Applying computer simulation, the single-step dynamic nature and the step-by-step paths for excitation transfer are investigated. The time constant and mean number of transfer events through a single-step provide a quantitative description of not only the dynamic property of each step but also the dominant pathways in phycobilisomes of blue-green algae. It is estimated that about 90% of the excitation energy is transferred to the core through β_{84} chromophores. The simulation also shows that the excitation energy is transferred in a natural phycobilisome most likely in partially reversible manner.

Keywords: Stochastic computer simulation; Excitation energy transfer; Phycobilisome; Single-step transfer ; Computer simulation; (Blue-green alga)

1. Introduction

The light-harvesting pigments in blue-green and red algae are concentrated mainly in phycobilisomes which attach to the thylakoid membrane. A phycobilisome of blue-green algae is comprised of an APC core and six C-PC rods which radially stretch from the core. Furthermore, each rod usually contains 1–4 hexamer disks of C-phycocyanins. Therefore, a PBS supramolecule may contain several hundreds of chromophores, among which more than a thousand energy transfer steps may be involved. Although the energy transfer processes in PBS are so complicated, the ultimate energy transfer efficiency in PBS can reach more than 90% [1,2]. This high efficiency of energy transfer has thus long been an important subject in photosynthetic studies.

The energy transfer in PBS was recognized many years ago from the steady-state spectra [3,4], by which not only the fact itself, but also the general pathway were suggested, i.e., PC → APC → Chl *a*. These were further confirmed later by the picosecond-level time-resolved spectra [5,6]; at the same time, the nature of this type of research was developed from qualitative to quantitative. However, because of currently available techniques and mathematical analysis methods as well as the inherent complexity of the system, to date it has been impossible to describe energy transfer kinetics in stepwise detail. It is, for instance, noted that the widely used data-fitting method with the exponential function suffers from the uniqueness problem [7]; on the other hand, the mathematically analyzed components could not reflect the real complexity of transfer processes [8]. These problems become even more serious for such a complex system as phycobilisome.

There has to date been plenty of research into the energy transfer processes in phycobilisomes, and, especially, picosecond-level time-resolved spectra clearly showed the sequence of C → PC → APC → Chl *a*. However, the transfer processes between the neighboring C-PC disks could not be observed directly: obviously, it is even more difficult to distinguish one transfer step from the others. There have been two types of theoretical model describing the energy transfer kinetics in phycobilisomes, one of which was the diffuse-limited model proposed by Glazer [2] and the other the trapping-limited model by Suter [9]. The former described disk-to-disk and disk-to-

Abbreviations: C-PC, C-phycocyanin; PBS, phycobilisome; s, sensitizer chromophore, β_{155}; f, fluorescer chromophore, β_{84}; m, intermediate chromophore, α_{84}; A.Q., *Agmenellum quadruplicatum* (a blue-green alga); M.L., *Mastigocladus laminosus* (a blue-green alga); ps, picosecond.

* Corresponding author. Fax: +86 2027837.

SSDI 0005-2728(94)00176-6

core transfers in equal rates, while the latter indicated that the disk-to-core step was the rate-limited one.

X-ray crystallography has provided detailed structural information of C-PC hexamers from several blue-green algae [9], therefore, it is now possible to construct a more exact model for energy transfer in the PBS. In the current work, energy transfer is explicitly considered chromophore-by-chromophore in a hexamer disk and also between the neighboring disks. Additionally, the function of linker polypeptides is considered in the model.

2. Model and method

In phycobilisomes, there are two physical factors to control the energy transfer kinetics from outer disk to central core, i.e., (1) the energy gradients existing between different types of pigment, such as those between PE and PC as well as PC and APC; (2) linker polypeptides, which modulate the absorption and fluorescence spectra of chromophores, make the energy gradients formed between same type of pigment (such as those between neighboring disks in a C-PC rod).

2.1. The simulation model

It is necessary to know the spectral properties of individual chromophores in order to understand the energy transfer processes occurring in a multichromophore system. Sauer and Mimuro have resolved the spectra of the three chromophores in a C-PC monomer [10,11]. The spectral data we used were kindly provided by Prof. Scheer in Germany and Prof. Sauer in the United States, and were resolved and used in their calculation of Förster transfer rates [10]. Recently, M.P. Debreczeny and Sauer et al. have convincingly resolved the absorption and fluorescence spectra of the three individual chromophore types found in the monomeric C-PC by applying the cpcB/C155S mutant, whose PC is missing the β_{155} chromophore, and a low-temperature technique, by which the absorption spectrum of the monomeric C-PC is partially resolved [12]. Using the modified spectral data, we have recalculated the spectral overlap integrals and the Förster rates for energy transfer in a C-PC hexamer. The impact of the changes on simulation results will be discussed in the last section of this paper.

The effect of linker polypeptides on spectra is considered based on the data published by Glazer [8]. The center-to-center distances and orientation factors between chromophores were reported in Ref. [13]. Using these data, the spectra overlap integrals and further Förster transfer rates are calculated; the transfer rates within a hexamer disk are directly taken from those reported by Sauer [14]. Because the crystal structure data of APC are still absent, the core is treated as an abstract trap. For the simulation model with an abstract core and a three-disk rod, there will be in total 251 reactions, 242 of which are for energy transfers and 9 for fluorescence emission from the three types of chromophore in the three disks.

The linker polypeptides between the neighboring C-PC disks modulate the absorption and fluorescence spectra of the chromophores, as reported by Glazer [8] and listed below.

	the third disk $(\alpha^{PC}\ \beta^{PC})_6L^{27}_{RC}$	the second disk $(\alpha^{PC}\ \beta^{PC})_6L^{33}_{R}$	the first disk $(\alpha^{PC}\ \beta^{PC})L^{30}_{R}$
λ_{max} (nm)	622.5	622.5	620.0
ε_{max} ($mm^{-1}\ cm^{-1}$)	2370	2370	2364
λ^{F}_{max} (nm)	652	648	643

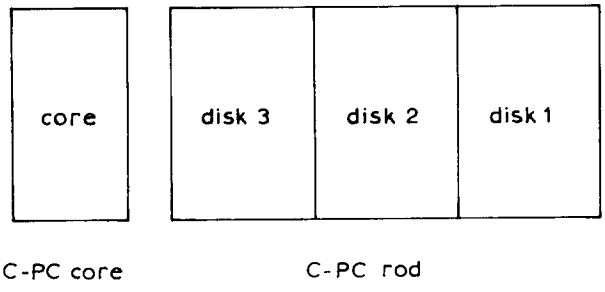

The experimentally obtained parameters for energy transfer from published papers are collected and listed in Table 1.

Obviously, the values could not be taken as the absolute foundation for evaluating a model, therefore, the transfer efficiencies and the average transfer events obtained from the simulation will also be used to evaluate the model.

2.2. The stochastic approach

With the simulation model, a stochastic simulation method, especially termed the Monte Carlo method, is applied to simulate the entire process from photon absorption to fluorescence emission through a series of energy transfer steps. Therefore, every step of the process become observable.

The theoretical basement and the rigorous deduction of the approach can be found in Ref. [20]; here, the general idea is described briefly. First of all, the discrete molecular numbers (or their combinations) are concerned instead of the continuous concentration in the deterministic approaches; additionally, the reacting probability constants are used instead of the deterministic reaction rate constants and defined in Eq. (1):

$c_u \mathrm{d}t$ = average probability that a particular combination of R_u reactant molecules will react accordingly in the next infinitessimal time interval $\mathrm{d}t$ (1)

Here C_u is the reacting probability constant, and the reactant combination is defined as:

h_u = number of distinct R_u molecular reactant combinations available in the state $(X_1, X_2, ..., X_N)$ for a system with X_1 molecules of species S_1, X_2 molecules of species S_2,..., and X_N molecules of S_N. (2)

According to Eqs. (1) and (2), the following relation is derived:

$a_u \mathrm{d}t = c_u h_u \mathrm{d}t$ = probability that an R_u reaction will occur in a system with volume V and the state $(X_1, X_2, ..., X_N)$ in the time interval $(t, t + \mathrm{d}t)$ at the time t (3)

If M reactions are involved in a system, each reaction will be set a reacting probability, i.e., a_u, $(u = 1,...,M)$, then the total reacting probability of the system will be:

$$a_0 = \sum_{u=1}^{M} a_u = \sum_{u=1}^{M} c_u h_u \tag{4}$$

Then, a function $P_0(\tau)$, defined as the probability that a system in the state $(X_1, X_2, ..., X_N)$ in the time interval $(t, t + \tau)$ would not undergo any reaction, is introduced without deduction:

$$P_0(\tau) = \exp\left(- \sum_{u=1}^{M} a_u \tau \right) = \exp(-a_0 \tau) \tag{5}$$

Now, for the system in the state $(X_1, X_2, ..., X_N)$ at time t, it turns out to be primarily to answer the two problems: when will next reaction occur, i.e., to determine τ; and what kind of the reaction will it be, i.e., to determine u.

In the stochastic simulation approach, two random numbers r_1 and r_2, which are distributed uniformly over the (0, 1) range, will be used to determine u and τ, then, from Eqs. (4) and (5), it will become apparent that:

$$\sum_{v=1}^{u-1} a_v < r_1 a_0 \leq \sum_{v=1}^{u} a_v \tag{6}$$

$$\tau = (1/a_0) \ln(1/r_2) \tag{7}$$

Then, u and τ can be determined according to Eqs. (6) and (7). Now, the algorithm can be practically used to simulate the stochastic time evolution of a reacting system. The simulation procedure is listed below:

step 1. Input the necessary values for the M reaction constants C_1, C_2,...,C_M and the N initial molecular population numbers $X_1, X_2, ...X_N$ for N types of reactants. Set reaction time t to zero. Initialize the unit-interval uniform random number generator.

step 2. Calculate and store the M quantities $a_1 = c_1 h_1$, $a_2 = c_2 h_2, ... a_M = c_M h_M$ for the current molecular population numbers, also calculate and store as a_0 the sum of the M a_v values.

step 3. Generate two random numbers, r_1 and r_2, using the unit-interval uniform random number generator, and calculate τ and u according to Eqs. (6) and (7).

Table 1
The lifetimes of fluorescence in the rod and the rise time of excitation energy in the core

Alga	Ref.	Disk mum./rod	t_{max}(ps)	τ_F(ps)
T. tennis (PE-less)	[15]	2	60	120
A. nidulans	[16]	2	60	160
Synechocystis sp.	[5]	2	83	
Synechococcus 6301 Mutant An112	[17]	1	45	
Synechococcus 6301 Mutant An112	[18]	3	83	
Synechococcus 6301 Mutant An112	[19]	4	120– 130	

step 4. Using the τ and u values obtained in step 2, increase t by τ, and adjust the molecular population levels to reflect the occurrence of one R_u reaction. Record each reaction pathway and the population of each species at regular intervals of time, as well as other desired information, then, if reactants vanish or the reacting time t reaches at the predetermined value, run to step 5, otherwise return to step 2 and repeat the $2 \rightarrow 3 \rightarrow 4$ loop.

step 5. Make many simulation runs from time zero to the chosen time t, corresponding to sampling randomly, with the initial states all identical except for the initialization of the random number generator. The number of runs should be more enough to obtain reasonable statistics in these estimates and will vary with the situation.

Specially for the purpose of the current work, it is proved that at least 10000 runs are needed to obtain reasonable simulation results.

From the simulation results for phycobiliproteins [21], it was learnt that the most informative parameters to show up the feature of stepwise energy transfer are time constants and mean number of transfer events. The time constants for a transfer step are obtained as following: record the time spent for a certain step, then, by statistics of the time, a plot of population to time is derived, from which the time constant can be obtained through fitting the curve with the monoexponential function, similarly for all other steps. The mean number of transfer events through a certain step for the excitation energy from a photon can be obtained similarly, i.e., record how many times for the excitation from a photon to travel through a path, and sum them for all absorbed photons and then find the arithmetic mean of the values. In this way, the average transfer events are obtained; do so for all other transfer steps.

The two types of parameter clearly show the feature of single-step transfer, i.e., the former estimates a transfer step in the view of time (or rate) while the latter estimates it in the view of quantity, i.e., it gives a measure of the probability or frequency and therefore the relative importance of the step in energy transfer.

From the simulation, the energy transfer efficiency, fluorescence lifetime in the rod and the excitation energy rising time in the core, and so forth, are also readily obtained.

2.3. The trapping rate of the core for excitation energy

The trapping rate of the core for the excitation energy can not be determined directly because the detailed structural information is still absent about the core and linkage of the core with the rod. Therefore, a trial parameter, k_{RC}, is used to simulate the trapping rate, i.e., it takes the values of 0.1, 0.3, 0.5 and 0.7 times k_d, which is the transfer rate from the first to the second disk. The simulation model contains a rod with 1–3 hexamer disks and an abstract core.

3. Simulation results

3.1. Förster transfer rates

The energy transfer between the chromophores in C-PC is assumed to occur by dipole–dipole interaction, usually named Förster transfer mechanism, and the rate is defined as the following [22].

$$k_T = \frac{9 \times \ln 10 K^2 \Phi_D}{128 \times \pi^5 n^4 \tau_D R^6} \int f_D(\nu) \varepsilon_A(\nu) \nu^{-4} d\nu \qquad (8)$$

Here, ν stands for wavenumber, $\varepsilon_A(\nu)$ is the extinction coefficient of the acceptor, $f_D(\nu)$ is normalized fluorescence spectra of the donor, N is the Avogadro constant, n is the refractive index, τ_d is the lifetime of the donor (when acceptors are absent), K is the orientation factor, R stands for center-to-center distance between the chromophores, and Φ_D is the quantum yield of fluorescence. The last term is the spectral overlap integral.

When linker polypeptides exist between the hexamer disks, the energy transfer between the disks could not be completely reversible but the forward transfer is more probable than the back one. Here, the transfer toward the core is defined as the forward transfer, while that away from the core is the back transfer. Because linker polypeptides are different in the various disks in a rod, so is their effect on the spectra of chromophores; therefore, the rates for the energy transfer from the first disk to the second are different from those from the second to the third. Linker polypeptides principally produce the effect on the spectra overlap integrals, which are listed in Table 2 for the three-disk model.

By the use of the integral values, as well as the data for R and K from [13] and Φ_D and n from Sauer [14], and τ_D with the value 1.5 ns^{-1}, the Förster transfer rates are calculated and listed in Table 3.

In the table, the transfer steps with the rates less than 1.0 ns^{-1} are omitted; in fact, only the paths of $5f \leftrightarrow 1f^*$, $6f \leftrightarrow 2f^*$, $4f \leftrightarrow 3f^*$ and those of $4m \leftrightarrow 1m^*$, $5m \leftrightarrow 2m^*$, $6m \leftrightarrow 3m^*$ are involved in the simulation model. The other paths are omitted because of the smaller rates.

Table 2
Spectra overlap integrals between the disks ($\times 10^{10}$, cm^6 mol^{-1})

Disk num.	Chromophore	Forward transfer			Back transfer		
		m	f	s	m	f	s
1st and 2nd	m	8.71	7.06	3.15	4.71	4.45	1.39
	f	7.65	6.45	2.60	3.93	3.83	1.13
	s	14.02	9.20	7.99	10.72	8.03	4.48
2nd and 3rd	m	6.95	6.02	2.27	5.64	5.14	1.73
	f	5.96	5.36	1.85	4.76	4.49	1.41
	s	12.92	8.92	6.48	11.79	8.52	5.33

Table 3
Förster transfer rates between the disks (ns^{-1})

1st disk ↔ 2nd disk			2nd disk ↔ 3rd disk		
k_T (left)	D-A pairs	k_T (right)	k_T (left)	D-A pairs	k_T (right)
134.62	5f ↔ 1f [a]	186.22	129.66	5f ↔ 1f [a]	154.84
14.93	4m ↔ 1m [a]	22.03	14.27	4m ↔ 1m [a]	17.58
10.25	6f ↔ 1m [a]	13.63	9.93	6f ↔ 1m [a]	11.62
6.43	6m ↔ 1f [a]	9.95	6.12	6m ↔ 1f [a]	7.67
5.79	5f ↔ 1s [a]	6.23	5.77	5f ↔ 1s [a]	6.04
2.65	6f ↔ 1s [a]	2.85	2.64	6f ↔ 1s [a]	2.76
2.52	6m ↔ 1s [a]	2.95	2.48	6m ↔ 1s [a]	2.72
1.82	6f ↔ 1f [a]	2.52	1.76	6f ↔ 1f [a]	2.10
1.56	6m ↔ 1m [a]	2.30	1.49	6m ↔ 1m [a]	1.84
1.18	6s ↔ 1s [a]	1.70	1.13	6s ↔ 1s [a]	1.38
0.67	5s ↔ 1f	1.17	0.63	5s ↔ 1f [a]	0.84

[a] The one nearer to core between two connected disks.

3.2. Some invariable parameters

The time constants for all the involved transfer steps possess only three distinct values related to the three types of donor, i.e., for the transfer steps with s, m and f chromophores as the donors, the time constants are 3.45 ps, 0.50 ps and 0.80 ps, respectively. Besides, these values would not change with the increase of disk number in the rod and of the trapping rates in the core. Another parameter, the fraction of the excitation energy transferred to the core through each pathway, is also shown to be invariable. From the simulation, it is shown that about 90% of the excitation entered the core through f chromophores and about 10% of that through m chromophores because f chromophores are located on the outer surface of the disks and nearest to the core.

3.3. The excitation decay in the rod and rise in the core

The excitation energy decay time in the rod and rise time in the core are listed in Table 4.

It is observed that the excitation rise time in the core is always shorter than the decay time in the rod, this phenomenon was experimentally observed [5]. From the simulation, it is noted that the excitation decay time in the various disks in a rod does not show observable differences. A possible reason is that the transfer between disks is very fast and at the same time occurrence of back transfers makes the decaying time indistinguishable in different disks; and another reason is that the data fitting method by multi-exponential function is used to obtain the fluorescence lifetime in the rod but is not sensitive enough to identify the difference in lifetimes among various disks.

Table 4
The parameters for the excitation decay in the rod (τ_F) and the excitation energy rise (t_{max}) (ps) in the core

	Time (ps)							
Parameter:	0.1 k_d		0.3 k_d		0.5 k_d		0.7 k_d	
Disk No.	τ_F	t_{max}	τ_F	t_{max}	τ_F	t_{max}	τ_F	t_{max}
1	217	28	80	10	46	6	30	1
2	344	60	155	50	105	35	95	40
3	454	160	220	100	175	90	155	80

Table 5
The efficiency for energy transfer (%)

Disk No.	Parameter:	0.1 k_d	0.3 k_d	0.5 k_d	0.7 k_d	1.0 k_d
1		85.1	94.1	96.5	97.3	98.0
2		75.2	88.0	91.7	93.2	94.0
3		67.7	82.3	86.4	88.0	89.0
Av. [a]		76.0	88.1	91.5	92.8	93.7

[a] Average obtained from arithmetic mean of the three values above.

3.4. The energy transfer efficiency

The efficiency is defined as the per cent of the excitation energy absorbed by the first disk is transferred to the core. The simulated transfer efficiencies are listed in Table 5 with 1–3 disks in the rod. Obviously, if the three disks in a rod absorb light evenly, the efficiency will be something between the calculated values and the average.

3.5. The mean number of transfer events through each step

The mean number of transfer events measures how many times the excitation from a photon has passed through a path before it is finally lost as fluorescence. They are listed in Tables 6, 7 and 8 for k_{RC} with the values of 0.3, 0.5 and 0.7 k_d, respectively.

From Table 6, it can be learnt that the transfer between the two chromophores in a fast-transfer pair still possesses the largest number of times; however, the absolute value is far smaller than that in C-PC trimer (about 288) and in

Table 6
The mean number of transfer events through each step with the trapping parameter 0.3 k_d

Donor	Acceptor	Single disk	Double disk		Three disks		
			disk 1	disk 2	disk 1	disk 2	disk 3
1s	1f	0.07	0.08	0.05	0.07	0.05	0.04
1f	1s	0.05	0.07	0.05	0.06	0.07	0.05
1m	1f	0.08	0.08	0.08	0.09	0.09	0.07
1f	1m	0.08	0.08	0.07	0.09	0.09	0.07
1m	2f	7.99	9.69	8.11	9.70	9.78	7.59
2f	1m	8.05	9.75	8.36	9.75	10.01	7.82
1m	4m	2.09	2.47	2.01	2.44	2.47	1.92
1s	6s	0.34	0.41	0.24	0.39	0.29	0.22
6s	1m	0.13	0.15	0.08	0.15	0.10	0.08
1m	6s	0.09	0.11	0.09	0.11	0.11	0.08
1m	6f	0.21	0.25	0.22	0.25	0.26	0.20
6f	1m	0.20	0.24	0.18	0.24	0.23	0.17
5f	1f [a]		1.20		1.42		1.13
1f [a]	5f		0.92		1.16		0.87
4m	1m [a]		0.10		0.13		0.10
1m [a]	4m		0.07		0.09		0.07

[a] The one nearer to the core between the neighboring disks.

Table 7
The mean number of transfer times through each step with the trapping parameter 0.5 k_d

Donor	Acceptor	Single disk	Double disks		Three disks		
			disk 1	disk 2	disk 1	disk 2	disk 3
1s	1f	0.05	0.06	0.03	0.07	0.04	0.03
1f	1s	0.04	0.05	0.04	0.05	0.05	0.04
1m	1f	0.05	0.07	0.05	0.08	0.07	0.05
1f	1m	0.05	0.07	0.05	0.07	0.07	0.05
1m	2f	5.17	7.52	5.37	8.18	7.65	5.06
2f	1m	5.49	7.57	5.61	8.24	7.89	5.28
1m	4m	1.34	1.93	1.38	2.08	1.93	1.30
1s	6s	0.26	0.33	0.16	0.36	0.23	0.15
6s	1m	0.10	0.12	0.06	0.14	0.08	0.05
1m	6s	0.06	0.08	0.06	0.09	0.09	0.05
1m	6f	0.14	0.20	0.15	0.21	0.20	0.14
6f	1m	0.12	0.18	0.11	0.19	0.18	0.11
5f	1f [a]		0.91		1.20		0.86
1f [a]	5f		0.63		0.91		0.58
4m	1m [a]		0.09		0.11		0.08
1m [a]	4m		0.05		0.08		0.04

[a] The one nearer to the core between the neighboring disks.

hexamer (about 143) The transfer from 1m to 4m possesses the largest number of times among the paths linking two trimers, while the transfer from 5f to 1f * is shown to be the dominant pathway between two neighboring disks.

As mentioned before, both the mean number of transfer times and the time constant reflect the nature of each transfer step. The latter evaluates a step in time, while the former measures it in frequency. However, there is a certain difference between them, i.e., time constants are classified into three values based on types of chromophore, while the mean number of transfer times reflects the nature of each step; therefore, this parameter measures the relative importance of a step.

Table 8
The mean number of transfer events through each step with the trapping parameter 0.7 k_d

Donor	Acceptor	Single disk	Double disks		Three disks		
			disk 1	disk 2	disk 1	disk 2	disk 3
1s	1f	0.04	0.06	0.02	0.07	0.04	0.02
1f	1s	0.03	0.04	0.03	0.05	0.04	0.03
1m	1f	0.04	0.06	0.04	0.07	0.06	0.04
1f	1m	0.04	0.06	0.04	0.07	0.06	0.04
1m	2f	4.04	6.58	4.25	7.61	6.92	4.05
2f	1m	4.24	6.62	4.50	7.67	7.15	4.28
1m	4m	1.02	1.68	1.11	1.94	1.75	1.04
1s	6s	0.22	0.31	0.12	0.33	0.20	0.11
6s	1m	0.09	0.11	0.04	0.12	0.07	0.04
1m	6s	0.05	0.07	0.05	0.08	0.08	0.04
1m	6f	0.10	0.18	0.11	0.20	0.18	0.11
6f	1m	0.09	0.16	0.08	0.18	0.15	0.08
5f	1f [a]		0.79		1.11		0.75
1f [a]	5f		0.51		0.83		0.48
4m	1m [a]		0.07		0.11		0.07
1m [a]	4m		0.04		0.07		0.04

[a] The one nearer to the core between the neighboring disks.

It can be seen from the three tables that the transfers between s and f chromophores as well as those between m and f in the same monomer become less important compared with those in phycobiliproteins. It also can be learnt that the transfers between neighboring disks and from the last disk to the core are principally through f chromophores. Estimated from the mean number of transfer times, about 90% of the excitation energy is transferred through f chromophores.

In comparison, the numbers of transfer times in phycobilisomes are far lower than those in phycobiliproteins because there are many more transfer pathways in PBS. Additionally, the core, playing a role of a trap, reduces the transfer times in the rod. From the data in the three tables, it can be seen that the mean number of transfers decreases with the increase in the trapping rate in the core, and among the disks, the one nearest to the core shows the least transfer events in Table 7.

4. Conclusion and discussion

4.1. The trapping parameters of APC core

It can be seen from Table 4 that the excitation decay time in the rod and rise time in the core would be closer to those in Table 1 if the trapping parameters are set between 0.3–0.5 k_d. The disagreement between the fluorescence lifetimes in the rod and the excitation rise time in the core may be due to the back-transfers between the disks and the smaller trapping parameter in the core compared with k_d. Table 9 shows that the τ_F and t_{max} would be much close if it is supposed that the back transfer is absent and the trapping parameter equals k_d and also the rod is longer (for instance, a rod with three disks).

The energy transfer efficiencies listed in Table 5 were less than those estimated experimentally [1,2] except for those with one-disk rod. From Table 9, if the excitation energy is supposed to be transferred irreversibly from outer disks to the core and the trapping parameter to be equal to k_d, the energy transfer efficiency would be similar to those reported in Ref. [2]. However, the decay and rise times in the one-way transfer model show large differences from those listed in Table 1. Besides, the linker polypeptides, which modulate the spectra of the chromophores in the disks, make the probability of the energy transfer toward core always larger than that away from the core but

Table 9
The fluorescence lifetimes in the rod, the rising time in the core and the transfer efficiency for the one-way transfer model

No. of disks	τ_F(ps)			t_{max}(ps)			Efficiency (%)		
	1.0 k	0.3 k	0.1 k	1.0 k	0.3 k	0.1 k	1.0 k	0.3 k	0.1 k
1	30	80	220	1	10	30	98	94	85
2	49	100	220	31	35	79	96	92	83
3	62	102	226	55	95	130	94	90	82

the back transfers would never be eliminated. To date, there have been few of the experimentally measured efficiencies available for phycobilisomes with various numbers of disks, and some of those were obtained only by rough estimation; on the other hand, in the simulation, the predetermined fluorescence lifetime is a crucial factor to determine the calculated efficiency: obviously, if the parameter is much smaller, the energy transfer efficiencies will be much higher. Besides, repeated transfer mechanism causes the quantum yield of fluorescence higher and therefore the energy transfer efficiency lower.

4.2. Excitation energy transfer

The nature of single-step transfer

A phycobilisome with a three-disk rod and an abstract core contains 64 chromophores and thousands of possible transfer steps. However, if only the interactions between the nearest neighboring chromophores are considered and further some less unimportant ones are omitted based on the experience in simulation on phycobiliproteins [21], there are 242 transfer paths involved in the current model. From the simulation, it is shown that the time constants for single-step transfers are classified to three types related to the transfers with s, m and f chromophores as donors. Specifically, the time constant is 3.45 ps for the transfers with s chromophores as the donors, 0.50 ps for those with m as the donors, and 0.80 ps with f as the donors; the probabilities for the excitation energy transferred through each step can be learnt from the mean number of transfer events listed in Tables 6–8.

The energy transfer within a trimer

There are three fast-transfer pairs linking the three monomers in a trimer, i.e., 1m ↔ 2f, 2m ↔ 3f and 3m ↔ 1f, in which the one-step transfer is completed in less than 1 ps. If an s chromophore is excited initially, the excitation energy will be preferably transferred to the f chromophore in the same monomer, from where it is most probably transferred to the m chromophore in the fast-transfer pair; repeatedly the excitation may transfer back and forth many times between the two chromophores in a fast-transfer pair, until, occasionally, it takes a less probable way into other chromophores or emit as fluorescence.

Table 10
The average transfer events in the fast-transfer pairs of the two trimers in a hexamer disk

Trimer no.	Pathway	One disk	Double disks		Three disks		
			disk 1	disk 2	disk 1	disk 2	disk 3
1	1m ↔ 2f	7.99	9.69	8.11	9.70	9.78	7.59
	2f ↔ 1m	8.05	9.75	8.36	9.75	10.0	7.82
2	4m ↔ 6f	7.53	9.15	7.03	9.24	8.69	6.67
	6f ↔ 4m	7.33	8.95	6.80	9.04	8.45	6.44

The energy transfer within a hexamer disk

According to the crystal structure, a hexamer is formed by two trimers face-to-face [13]. Therefore, six f chromophores in a hexamer are located on the outer surface of the hexamer, while s and m chromophores are located at the inner. It is estimated from the mean number of transfer events that up to 70–80% of the excitation is transferred through m chromophores, and 10–20% through the s chromophores, while only less than 10% is transferred through f chromophores. In fact, in a trimer, f chromophores play a role of 'energy reservoir' and provide energy for m chromophores from which the excitation is transferred to another trimer. This feature can be easily observed from Table 10.

For example, it can be seen that 2f → 1m involves many more transfer events than 1m → 2f because excitation energy is transferred predominantly through m chromophores to another trimer. Evaluated by the number of transfer events, the 1s ↔ 6s, 2s ↔ 4s and 3s ↔ 5s paths are much more effective than s → f within a monomer. In this case, the excitation energy at an s chromophore would be preferably transferred to an s chromophore in another trimer instead of taking the s → f path within a monomer.

The energy transfer between disks

As mentioned before, the most probable ways for energy transfers between the neighboring disks are those through the f chromophores. The simulation shows that about 90% of the excitation energy is transferred through f

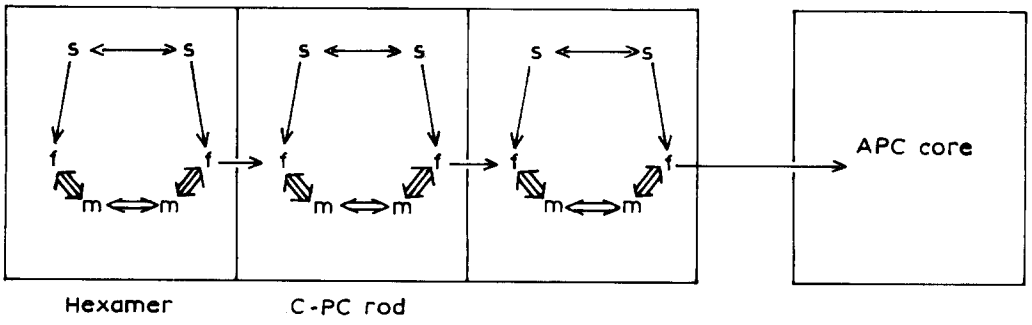

Fig. 1. Illustration for energy transfer in the phycobilisomes.

chromophores. This feature is also can be seen from Table 10. In the second trimer, the path of 4m → 6f involves many more transfer events than that of 6f → 4m because m chromophores play the role of 'energy reservoir' in turn.

The energy transfer in phycobilisomes

It can be seen from the crystal structure of C-PC hexamer that the periodic repeating units are the hexamers instead of the trimers, so these are the route for energy transfer along the rod. As mentioned before, the dominant pathways for energy transfer between the two trimers in a disk are m ↔ m paths and f chromophores play a role of 'energy reservoir'; while those between two neighboring disks are f ↔ f paths, in turn, m chromophores as 'energy reservoir'. In addition, f chromophores are also responsible for transferring the excitation to the APC core. Fig. 1 shows the principal routes for energy transfer along the rod into the APC core.

The structure of a phycobilisome and the dominant pathways for energy transfer are illustrated in Fig. 2, in

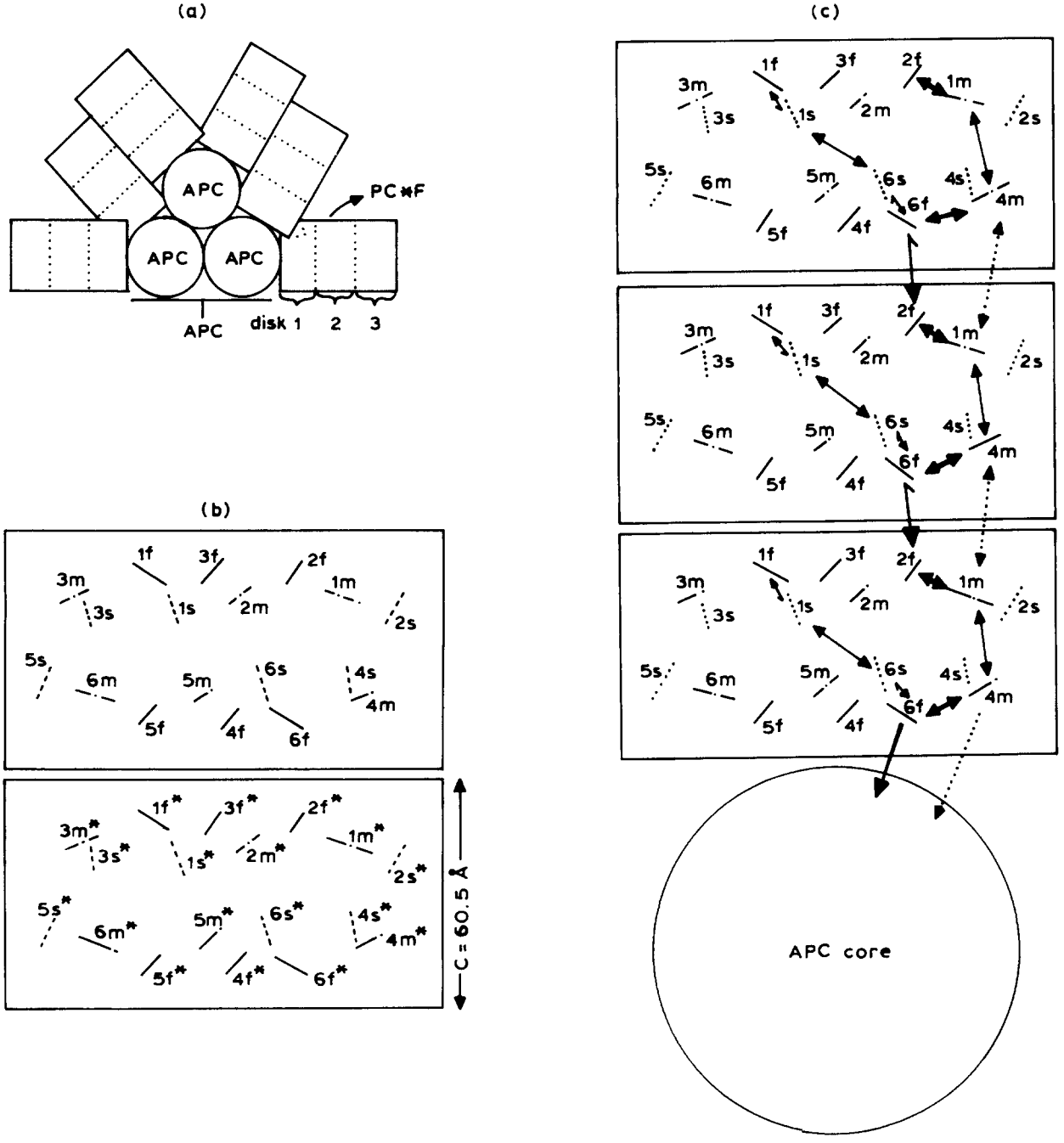

Fig. 2. The structure of a phycobilisome. (a) The spacial position of chromophores in the rod (b) and the dominant pathways for energy transfer. –, f; —, s; – · –, m chromophores.

Table 11
The spectral overlap integrals ($\times 10^{10}$, cm^6 $mol-1$)

Acceptor donor	Calc. [a]	m		f		s	
			D%		D%		D%
m	o	7.58	18	6.39	32	2.57	81
	n	8.94		8.41		4.64	
f	o	6.56	−18	5.75	8	2.10	−0.4
	n	5.41		6.23		2.09	
s	o	13.27	16	8.97	30	7.01	63
	n	15.41		11.66		11.44	

[a] o: calculated with the old spectral data, n with the new ones.

which the structures of a hexamer are obtained from Ref. [13].

According to the crystal structure of the C-PC hexamer, there should be three symmetrical pathways; in the figure only one of them is shown.

The effect of the modified spectral data on simulation results

By using data published by Debreczeny and Sauer, we recalculated the spectral overlap integrals and Förster transfer rates in a C-PC hexamer. the values and relative changes from the old ones are listed in Tables 11 and 12.

In Tables 11 and 12, *D%* means percent of difference of values calculated with the old and the new spectral data.

From Eq. (8) it is known that the changes on spectral data could only produce an effect on the overlap integral term of the rate. Generally, the new spectral data enlarge the overlap integrals except for those between f and s chromophores as well as between f and m chromophores as the donor and the acceptor, respectively. However, the rates calculated with new spectral data are without exception larger than those with the old ones, for the fluorescence quantum yield is also increased [10,12]. In comparison, the overlap integrals change most for the pairs with m and s as the donors and s as the acceptor; however, the absolute value of the rate is very low for the transfer from m to s, whereas for the transfer from an s to another s (such as from 1s to 6s), it has already proved to be the most important among the transfer paths, with the s as the donor based on the calculation with the old data. Therefore, the new spectral data could only change the absolute values of certain parameters, but would not change the sequence of the order of transfer pathway, among which the time constants would change most, for example, the time constant for the transfers with s as the donors will reduce to about 2 ps from 3.45 ps; from 0.5 ps to around 0.4 ps for the transfer paths with the m as the donors, while that with f would not change much. Therefore, it is reasonable to conclude that the new spectral data will not introduce any alterations in the general conclusion from the simulation.

In the current work, the core has been treated as an abstract trap, i.e., once the excitation energy gets into the core, it will never return to the rod. In fact, it is generally accepted that the excitation energy will be immediately transferred into the final emitter, F_{680}, after it enters into the core; therefore, it is quite reasonable to consider the core as an abstract trap. In addition, the significant difference in the spectra of C-PC and APC suggests inhibition of the back transfer from the core to the rod.

Stochastic computer simulation techniques can directly trace, observe and record detailed information, and via statistics gained from microscopic quantities, macroscopic results comparable with experimental ones can be derived.

Table 12
The Förster rates (ns^{-1}) for energy transfer in a C-PC hexamer

D%	k (F → E)		Chromophores		k (E → F)		D%
	new	old	E	F	old	new	
3	10.55	10.22	1m ↔ 1f		14.94	19.68	32
24	8.45	6.81	1s ↔ 1f		43.59	62.15	43
80	0.92	0.51	1s ↔ 1m		2.63	3.35	27
3	1159.95	1123.57	1m ↔ 2f		1642.10	2162.86	32
35	13.40	9.89	1f ↔ 2f		9.89	13.40	35
18	448.91	380.10	1m ↔ 4m		380.10	448.91	18
79	424.23	236.76	1s ↔ 6s		236.76	424.23	79
81	29.41	16.28	1s ↔ 6m		84.09	107.14	27
			1m ↔ 6s				
3	30.91		1m ↔ 6f		43.76	57.64	32
		29.94	1f ↔ 6m				
35	16.02	11.83	1f ↔ 6f		11.83	16.02	35
24	2.26	1.82	1s ↔ 6f		11.66		43
			1f ↔ 6s			16.63	
35	6.77	5.00	1f ↔ 4f		5.00	6.77	35
35	13.55	10.00	1f ↔ 5f		10.00	13.55	35
24	0.92	0.74	1s ↔ 5f		4.74	6.76	43
			1f ↔ 5s				

Acknowledgements

This project was supported by the National Natural Science Foundation of China.

References

[1] Grabowski, J and Gantt, E. (1978) Photochem. Photobiol. 28, 47.
[2] Glazer, A.N., Yeh, S.W. and Webb, S.P. and Clark, J.H. (1985) Science 227 (1985) 419–423.
[3] Duysens, L.N.M. (1951) Nature 158, 548.
[4] Gantt, E. and Lipschults, C.A. (1973) Biochim. Biophys. Acta, 292, 858.
[5] Yamazaki, I., Tamai, N., Yamazaki, T., Murikami, A., Mimuro M. and Fujita, F. (1988) Phys, J. Chem. 92, 5035–5044.
[6] Mimuro, M., Yamazaki, I., Tamai, N. and Katoh, T. (1989) Biochim. Biophys. Acta 973, 153–162.
[7] Isenberg, I., Dyson, R.D. and Hanson, R. (1973) Biophys. J. 13, 1090–1115.
[8] Glazer, A.N. (1985) Annu. Rev. Biophys. Biophys. Chem. 14, 47–77.
[9] Suter, G.W. and Holzwarth, A.R. (1987) Biophys. J. 52, 673–683.
[10] Sauer, K., Scheer, H. and Sauer, P. (1987) Photochem. Photobiol. 46, 427–440.
[11] Mimuro, M., Fuglistaller, P., Rumbell, R. et al. (1986) Biochim. Biophys. Acta 848, 155.
[12] Debreczeny, M.P., Sauer, K., Zhou, J.H. and Bryant, D.A. (1993) J. Phys. Chem. 97, 9852–9862.
[13] Schirmer, T., Bode, W. and Huber, R. (1987) J. Mol. Biol. 195, 677–695.
[14] Sauer, K. and Scheer, H. (1988) Biochim. Biophys. Acta 936, 157–170.
[15] Mimuro, M., Yamazaki, I., Yamazaki, T. and Fujita, Y. (1985) Photochem. Photobiol. 41, 597-603.
[16] Yamazaki, I., Mimuro, M., Murao, T., Yamazaki, T., Yashihara, K. and Fujita, Y. (1984) Photochem. Photobiol. 39, 233-240.
[17] Gillbro, T., Sandstrom, A., Sundstrom, V., Wendler, J. and Holzwarth, A.R. (1985) Biochim. Biophys. Acta 808, 52-65.
[18] Gillbro, T., Sandstrom, A., Sundstrom, V. and Holzwarth, A.R. (1983) FEBS Lett. 162, 64-68.
[19] Suter, G.W., Mazzola, P., Wendler, J. and Holzwarth, A.R. (1984) Biochim. Biophys. Acta 766, 269-276.
[20] Gillspie, D.T. (1977) J. Phys. Chem. 81, 2340–2361.
[21] Zhao, J.Q., Zhu, J.C. and Jiang, L.J. (1994) (a) Science in China (series B), 37, 831–841; (b) 37, 1313–1320.
[22] Förster, T. (1967) in Comprehensive Biochemistry (Florkin, M. and Stotz, E.H., eds.), Vol. 2, Ch. 2, pp. 61–80, Elsevier, Amsterdam.